



A field focusing butterfly stripline detects NMR at higher signal-to-noise ratio



Yen-Tse Cheng, Jan G. Korvink*, Mazin Jouda*

Karlsruhe Institute of Technology (KIT), Institute of Microstructure Technology, Karlsruhe 76131, Germany

ARTICLE INFO

Article history:

Received 20 February 2023

Revised 23 June 2023

Accepted 25 June 2023

Available online 29 June 2023

Keywords:

Stripline detector

High SNR

Radiofrequency shielding

Parallel MR

ABSTRACT

We present a compact tuned magnetic resonance detector that merges the conductor topology of a butterfly coil with that of a stripline, thereby increasing the magnetic field intensity B_1 per unit current, which increases the detection signal-to-noise ratio for mass-limited samples by a factor of 2. The s-parameter measurements further reveal improved radiofrequency shielding through the suppression of B_1 outside the coil when operated within an array of similar detectors. Simulations additionally show a sharper B_1 fall-off for the butterfly stripline outside the sensitive sample region. Our design is compatible with 2D planar manufacturing procedures, such as printed circuit board technology, and surface micromachining.

© 2023 The Author(s). Published by Elsevier Inc. This is an open access article under the CC BY-NC-ND license (<http://creativecommons.org/licenses/by-nc-nd/4.0/>).

1. Introduction

NMR is a robust tool for informative biochemical analysis covering a broad range of applications, such as drug screening, protein folding, or discovery of natural byproducts [4,12,14]. In recent years, there has been an increasing interest in hardware design for high throughput NMR, especially for parallel coil arrays [3,7,21]. Obtaining spectra simultaneously from a large number of individual receive elements requires a highly isolated detection environment. Another key requirement is to enhance the sensitivity in the region of interest, which nudges research towards finding micro coils with a high-quality factor Q .

Hence, seeking the best coil topology to implement in a coil array has brought our attention to stripline-based coils [16] and microslot detectors [8], due to their high sensitivity and their inherited RF shielding. The microslot detector was developed by Maguire et al. [8], which scaled down the sample volume to sub-millimeter dimensions, i.e., by more than a factor of 3,500 compared to a conventional 5 mm sample tube. The planar structure of the stripline makes it a strong candidate for many applications, such as in situ electrochemical NMR [19], in-line chemical reaction monitoring [20], geometrically-differential NMR detection [16], or net-phase flow NMR [17]. Additionally, the dual-layer construction, in which one layer is a ground plane, offers a high degree of RF shielding, making it ideal for MR high-throughput arrays.

Previous publications [1,18] have shown that an electrically highly isolated coil array allows for less signal coupling, removing the need for complex decoupling schemes involving low-impedance preamplifier front-ends [15].

Minute sample quantities, such as individual biological cell clusters, precious biopsies, or bio-active materials which cannot be obtained in large quantities, require a refined mass-limited regime where spins of the sample can be detected with sufficient SNR by the MR sensor. Utilizing a micro-coil combined with a microchannel [10] is one of the solutions for such applications with very low detection limits. Unlike the typical solenoid coils, the stripline is restricted to one loop structure, which limits its sensitivity. Another shortcoming of stripline coils is their intrinsically low inductance, requiring larger capacitance to form a resonating circuit, which makes it difficult to integrate with CMOS-based receivers for low-field magnets.

This paper presents a new stripline design that produces a stronger and more concentrated RF field through a unique butterfly-shaped strip. It improves upon the SNR of a regular stripline when targeting mass-limited samples, which otherwise would result in a low sample filling factor. The presented design improves B_1 shielding, and achieves B_1 suppression outside the detection region of the stripline, while boosting the detector's sensitivity.

2. Resonator design

Based on Bart et al. [2], the geometric parameters of the regular stripline (RS) have been optimized to achieve the best MR

* Corresponding authors.

E-mail addresses: jan.korvink@kit.edu (J.G. Korvink), mazin.jouda@kit.edu (M. Jouda).

performance. Particularly, the SNR is found to reach an optimum when the aspect ratio (the ratio of the length of the sensitive part to its width) is 5. Moreover, it is widely accepted that unwanted spectral spreading mainly originates from magnetic susceptibility jumps at material interfaces crossing the direction of the \mathbf{B}_0 field. That is one reason why saddle coils are preferable to solenoidal coils in high-resolution applications. Therefore, we retain the sandwich structure of a regular stripline, with an aspect ratio of 5, to achieve an optimal SNR, and to avoid the effects of susceptibility artifacts.

Fig. 1 shows the transformation of a regular stripline into a butterfly stripline, for which the center sensitive conductor stripe was replaced by two identical and parallel loop coils, denoted by L_1 and L_2 . Both coils carry the same current, and their layout allows the currents to flow oppositely, resulting in a \mathbf{B}_1 field perpendicular to the \mathbf{B}_0 experienced by the sample. The ground plane, besides providing RF shielding, helps to homogenize the \mathbf{B}_1 field in the region of interest. The contribution of the butterfly stripline is to reach beyond the sensitivity limits of the conventional stripline, by allowing to add as many loops as practicable, as long as the self-resonance frequency is maintained sufficiently high.

The signal-to-noise ratio (SNR) after a 90° pulse is a measure of the quality of the RF detector as stated by Hoult and Richards [5] in what is known as the principle of reciprocity. It is given by [13]

$$\text{SNR} = \left(\frac{|\mathbf{B}_1|}{i}\right) \cdot \frac{k_0 v_s N h^2 I(I+1) \omega_0^2 / 3 \sqrt{2} k_B T}{V_{\text{noise}}} \quad (1)$$

$$\propto \left(\frac{|\mathbf{B}_1|}{i}\right) \cdot \frac{1}{\sqrt{R}}$$

In Eq. 1, $|\mathbf{B}_1|/i$ is the magnetic field per unit current i at the Larmor spin precession frequency ω_0 , k_0 is a constant to account for the \mathbf{B}_1 inhomogeneity, while V_{noise} is the noise voltage associated with the signal and is mainly dependent on the coil's resistance at the Larmor frequency, $v_s N$ represents the number of spins involved, I is the spin quantum number, and k_B and h are the Boltzmann and Planck constants. Assuming a uniformly filled sample in the coil, as well as a homogeneous \mathbf{B}_1 , the SNR and coil's signal detection quality, by definition, is then defined by the coil's field per unit current per square root of its resistance.

In light of Eq. 1, one can comprehend the superior sensitivity of the proposed butterfly coil by referring to Fig. S1, see "Supplementary material", which illustrates its considerably higher current density compared to the regular stripline when the same current

flows in both coils. It results from the small cross-section of the wires, leading to a stronger \mathbf{B}_1 field in the sample region.

2.1. FEM simulation

To find a suitable butterfly stripline geometry, we parameterized the dimension of the butterfly stripline, as shown in Fig. 1b. The design parameters that define the coil are the trace width w and the space s between traces. Parameters are swept to reasonable values while avoiding the merging of copper traces. The separation between the stripline and ground plane is fixed to a uniform distance of $500 \mu\text{m}$. Electromagnetic simulations are performed with a commercial finite element package (COMSOL Multiphysics 5.4, RF modules, COMSOL AB, Sweden) to reveal their performance for the excitation efficiency, and to achieve the estimated MR response. Each component in the simulation model is a three-layer stacked structure comprising two metal planes (stripline and ground), sandwiching a sample-carrying capillary. Each coil is excited at a uniform lumped port with an input current of 1A.

Fig. 2a and Fig. 2b display normalized contour plots of the simulated \mathbf{B}_1 map over the central cross-section of the coil for the regular and butterfly stripline. The results indicate that the \mathbf{B}_1 at the region of interest of the butterfly stripline is $7\times$ that of the regular stripline, which is significantly higher due to the higher current density in its wires and the confinement of its RF field. The \mathbf{B}_1 intensity below the sensitive section decays at the same rate for both coil structures along the vertical z -direction, as seen from the 2% \mathbf{B}_1 iso-lines (yellow), also the field above the ground plane in both cases is almost negligible. Furthermore, the iso-line at the edge of the butterfly stripline is much narrower than that of the regular stripline, highlighting its superior field shielding and field concentration at the position of the sample. The result can be explained by the cancellation of the field generated from the center and outer loops of the butterfly structure in which the counter-currents ensure less field leaking from the edges. Based on a modified Wheeler formula [11] for planar spiral coils, the inductance increases quadratically with the number of windings, thus achieving stronger RF fields by adding more windings. For comparison, we simulated a single-loop and a double-loop butterfly stripline as depicted in Fig. 2c, which indicates how the \mathbf{B}_1 field in the sensitive area is positively correlated with the number of turns. Also as

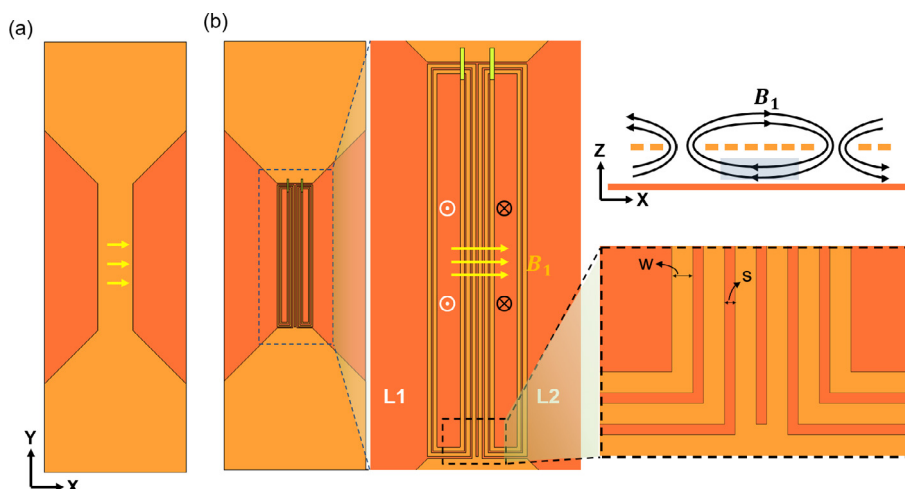


Fig. 1. The regular and butterfly stripline coils possess a ground plane for RF shielding and produce their \mathbf{B}_1 field perpendicular to the \mathbf{B}_0 -direction. The coils are parameterized by the trace width w and separation between traces $s = w/2$ for the simulation results in Figs. 2 and 3. (a) Layout of a regular stripline. (b) The new butterfly-stripline design schematically illustrates the \mathbf{B}_1 field streamlines and important geometrical parameters.

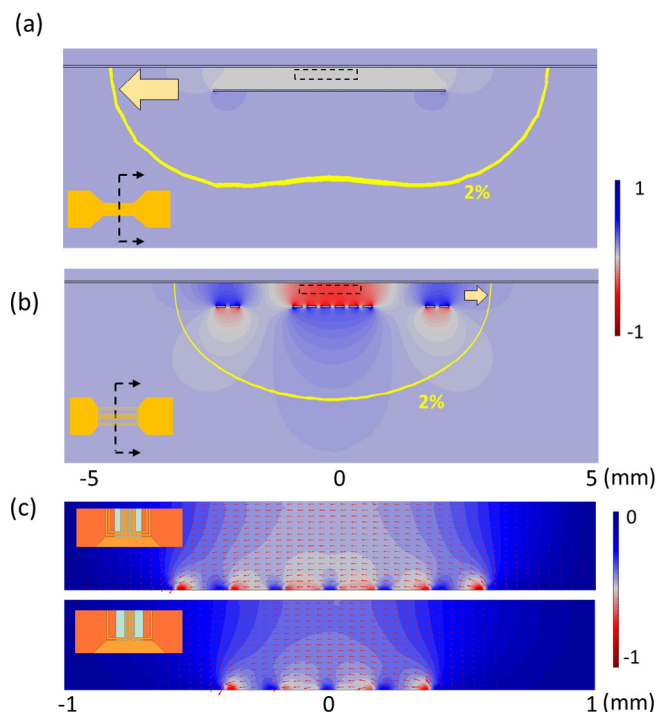


Fig. 2. Cross-sectional RF field plot at the center of (a) a regular, and (b) a butterfly-stripline coil. (c) B_1 field plots comparing a single and a two-loop butterfly stripline coil at the center cross section (frequency: 45 MHz).

indicated in Fig. S2, we found that a higher B_1 strength can also be attained by reducing the dimension of the looped coils. We further calculated the SNR based on the simulation data, as seen in Table S1, showing a maximum SNR enhancement of more than $2.76\times$.

An ideal stripline coil should only produce a concentrated magnetic field in the sensitive central region of the strip (the narrow part) and a negligible field at both lateral edges. One important motivation is that the lateral B_1 field could overlap with undesired

sample regions, where the B_0 field's homogeneity might be compromised, and thus would result in an unwanted tail in the NMR spectrum. Furthermore, the stripline pads are usually connected closely to a tank circuit to avoid the large parasitic inductance from the extension traces, which is comparable to the inductance of the narrow part of stripline coil. Thus increasing the inductance of the stripline relaxes this constraint and renders the effect of parasitic inductance negligible. Ideally, the sample should only overlap with the strip, but for facile sample handling it would be better to deliver the sample through a long channel to minimize susceptibility

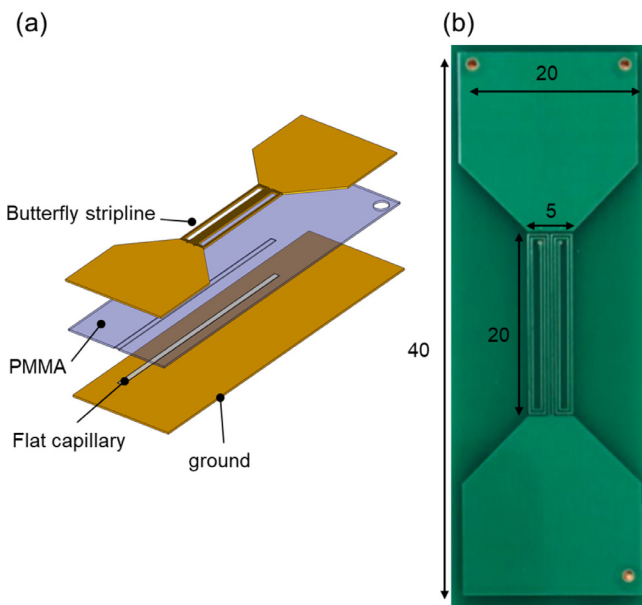


Fig. 4. (a) The schematic assembly of a butterfly device starts with a top stripline, a PMMA spacer, a flat capillary, and a bottom ground plate. (b) The photo depicts a double-loop butterfly stripline, with $200\ \mu\text{m}$ wide copper tracks, and a $100\ \mu\text{m}$ gap separating the conductor stripes. The two upper vias shown in the photo are used to connect the stripline to the bottom ground plate. All units are in [mm].

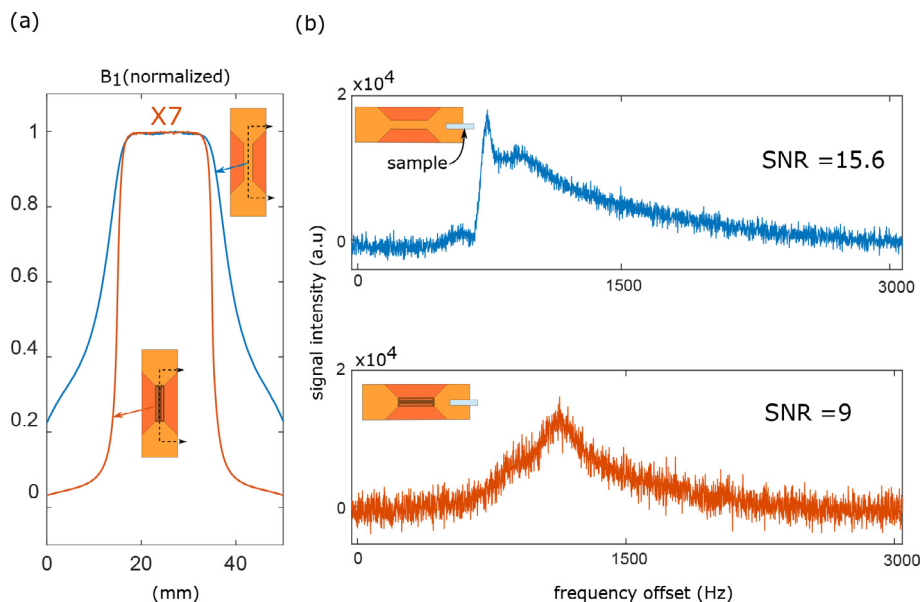


Fig. 3. (a) Simulation of the B_1 distribution along a regular (blue) and butterfly (orange) stripline. The butterfly stripline has a 7-fold higher B_1 compared to the regular stripline. (b) Averaged MR spectrum (10 scans) from a sample located at the pad for a regular stripline, and a butterfly coil. The latter exhibits a stronger suppression of the sample outside the sensitive region.

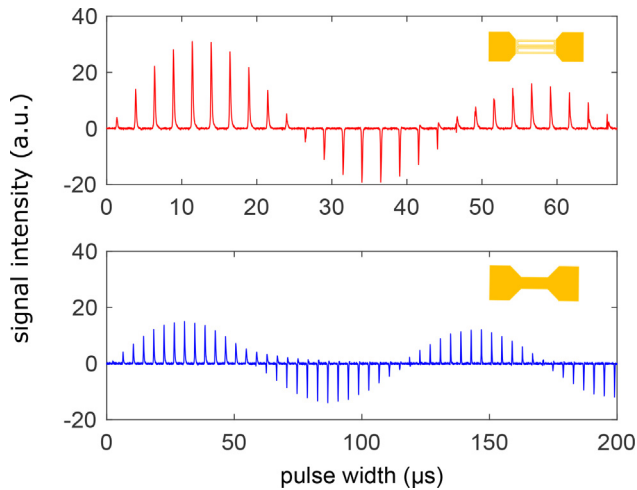


Fig. 5. ¹H Nutation curves of a two-looped butterfly stripline coil (red) and a regular stripline coil (blue). Both coils have the same geometrical footprint, and are excited with 1 W.

artifacts resulting from the sample-to-air interface. For this purpose, we simulated the B_1 field in the sample region of both coils along the y-axis, as shown in Fig. 3a. The butterfly-stripline exhibits, as depicted, a sharper decay of the B_1 field towards the wider part of the coil, resulting in a lower contribution of this part of the sample to the MR signal. The superior advantage of the butterfly coil in suppressing the sample excitation outside the sensitive region was verified experimentally, as illustrated in Fig. 3b, by comparing the sensitivity of the two coils to a 1 μ L H₂O sample placed at the stripline pad, while exciting both coils at 90° flip angle. SNR is reduced from 15.6 to 9.

3. Coil fabrication and experimental result

Based on the simulation results, both the double-loop butterfly and a regular stripline were selected for comparison. The two coils were fabricated using a commercially available PCB technology, and each resonator comprised three layers, a stripline, a PMMA spacer, and a ground plane, as illustrated in Fig. 4a. Each coil was fabricated with an overall length of 40mm, and a width of 20mm, with a sensitive conductor section of 20 mm \times 5 mm. A PMMA spacer of 0.5 mm was cut with a 1 mm wide channel using a CO₂ infrared laser cutter. A sample solution of 50mM CuSO₄ in water was introduced in a flat capillary (thickness: 0.1 mm, width: 1 mm), corresponding to a 2 μ L volume, which was then inserted in the pre-cut PMMA spacer. After assembly, the resonators were tuned and matched using a network analyzer (E5071C, Agilent), using nonmagnetic capacitors (model 5641, Johanson Manufacturing, NJ), to the ¹H Larmor frequency, corresponding to 45 MHz. Both coils were tested in a pre-clinical 1.05 T cryogen-free MRI magnet system (Bruker Biospin, Ettlingen, Germany).

One experiment that can evaluate the performance of the butterfly coil, and compare it with the regular stripline, is to measure the nutation curve of the two coils. The ¹H nutation signals for both coils are depicted in Fig. 5. According to these results, the maximum MR signal intensity (around 15 [a.u.]) for regular stripline was achieved at an excitation pulse of $\tau = 30 \mu s$ and the B_1 uniformity at 45°/90° ratio is around 80%. On the other hand, the butterfly coil showed a maximum signal intensity of 31 [a.u.] at an excitation pulse duration of $\tau = 11 \mu s$. Both coils were excited with 1 W. Even though the 45°/90° is decreased to 51%, the result indicates a large $\sim 2\times$ improvement of SNR, and a $\sim 2.7\times$ reduction in the 90° pulse duration.

An acceptable signal coupling below -20 dB for two spaced coils has been used as a standard requirement for an MRI array with a decoupling scheme [6]. Although it is possible to utilize

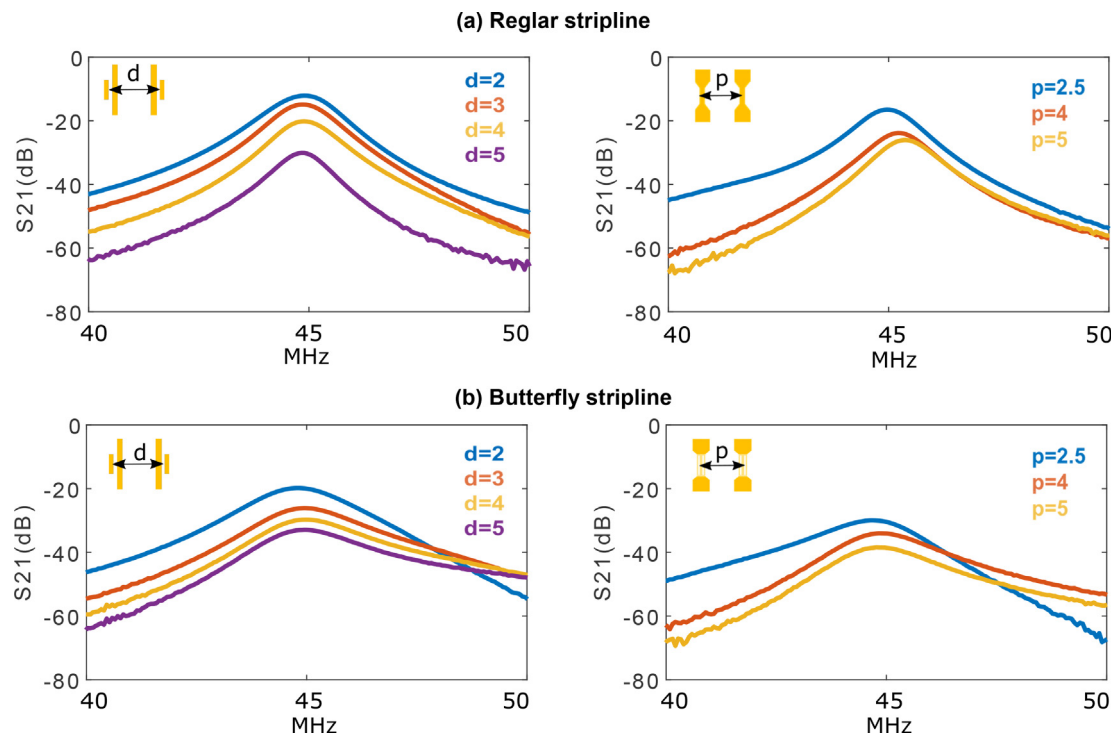


Fig. 6. (a) Coupling coefficients for two regular stripline coils resonating at 45MHz, for different back-to-back distances, ranging from 2 cm to 5 cm, with S_{21} varying from -12.25 dB to -30.65 dB, and side-by-side distances from 2.5 cm to 5 cm, with a corresponding S_{21} varying from -16.54 dB to -27.75 dB. (b) Coupling coefficients for two butterfly stripline coils resonating at 45MHz, for the same back-to-back distances with S_{21} varying from -20.04 dB to -32.96 dB, and same side-by-side distances with S_{21} varying from -30.51 dB to -38.62 dB.

techniques such as active decoupling to reduce the crosstalk further, it is still necessary to maintain the geometrical coupling of the coils as low as possible. As indicated in the simulation result, the butterfly-stripline exhibits a relatively more confined RF field map than the regular stripline at the narrow region of the sensitive section. To verify this, four coils (two copies of the regular stripline and two copies of the butterfly coil) were tuned to 45 MHz and matched to 50Ω at the bench, with a scattering parameter S_{11} less than -15dB . The coupling coefficient S_{21} of an array of two similar coils was measured while varying the distance between the coils for two scenarios, once placed back-to-back, and once placed side-by-side. Figs. 6a and 6b summarize the results for the two stripline arrays. Compared to the regular stripline, the butterfly exhibits a stronger coupling suppression of 7.79 dB to 2.31 dB for a back-to-back distance range $d \in 2\text{ cm}$ to 5 cm. Also, a stronger signal decoupling range of 14 dB to 10.87 dB is achieved by the butterfly topology for a side-by-side separation in the range $p \in 2.5\text{ cm}$ to 5 cm. The result can be explained from the distribution of the \mathbf{B}_1 field, see Fig. 2a,b. The elliptical shape of the butterfly coil's \mathbf{B}_1 field has a lower horizontal stray field than the saddle-shaped field of the regular stripline, leading to a stronger suppression of coupling.

4. Conclusion

We have presented a method with which to boost the sensitivity of a regular stripline when its filling factor is low due to limited sample mass. The idea, that is based on replacing the sensitive part of a regular stripline with a multi-loop butterfly coil, yielded a factor 2 enhancement in sensitivity, and a 14 dB lower coupling when the coil was used in an array configuration. Furthermore, the FEM simulations showed a sharper \mathbf{B}_1 suppression outside the region of interest compared to the regular stripline. The proposed design additionally offers a major advantage of design flexibility where the butterfly structure can be freely optimized, in terms of geometry and number of loops, to achieve arbitrary \mathbf{B}_1 profiles. For instance, an asymmetric butterfly structure could be used to produce a linear \mathbf{B}_1 gradient along any axis for \mathbf{B}_1 -gradient coherence selection [9].

In the present study, the butterfly stripline has not yet been exploited in an array for high-resolution parallel MR detection. Nonetheless, its enhanced shielding, confirmed from simulation and experimental results, makes it a good candidate for parallel MR experiments [3], due to the self-cancellation of the RF field away from the stripline. This guarantees not only less signal coupling to neighboring detector units but also a more dense arrangement of the array.

Data availability

Data will be made available on request.

Declaration of Competing Interest

The authors declare the following financial interests/personal relationships which may be considered as potential competing interests: [Jan G. Korvink reports a relationship with Voxalytic GmbH that includes: board membership.]

Acknowledgments

This research was funded by the Deutsche Forschungsgemeinschaft (DFG, German Research Foundation) under Grant No.

389084717 (ScreeMR). JGK and MJ additionally acknowledge support from the ERC Synergy Grant under Grant No. 951459 (HiSCORE). Both projects are managed under the Helmholtz Program Material Systems Engineering, topic 5 (Materials Information Discovery).

All authors acknowledged support from the KIT-Publication Fund of the Karlsruhe Institute of Technology.

Appendix A. Supplementary material

Supplementary data associated with this article can be found, in the online version, at <https://doi.org/10.1016/j.jmr.2023.107517>.

References

- [1] G. Adriany, P.F. Van de Moortele, F. Wiesinger, S. Moeller, J.P. Strupp, P. Andersen, C. Snyder, X. Zhang, W. Chen, K.P. Pruessmann, et al., Transmit and receive transmission line arrays for 7 Tesla parallel imaging, *Magn. Reson. Med.*: Off. J. Int. Soc. Magn. Reson. Med. 53 (2005) 434–445.
- [2] J. Bart, J. Janssen, P. Van Bentum, A. Kentgens, J.G. Gardeniers, Optimization of stripline-based microfluidic chips for high-resolution NMR, *J. Mag. Reson.* 201 (2009) 175–185.
- [3] Y.T. Cheng, M. Jouda, J. Korvink, Sample-centred shimming enables independent parallel NMR detection, *Sci. Rep.* 12 (2022) 1–9.
- [4] H.J. Dyson, P.E. Wright, Unfolded proteins and protein folding studied by NMR, *Chem. Rev.* 104 (2004) 3607–3622.
- [5] D.I. Hoult, R. Richards, The signal-to-noise ratio of the nuclear magnetic resonance experiment, *J. Magn. Reson.* 1969 (24) (1976) 71–85.
- [6] M. Kozlov, R. Turner, Analysis of RF transmit performance for a 7T dual row multichannel MRI loop array, in: 2011 Annual International Conference of the IEEE Engineering in Medicine and Biology Society, IEEE, 2011, pp. 547–553.
- [7] K.M. Lei, D. Ha, Y.Q. Song, R.M. Westervelt, R. Martins, P.I. Mak, D. Ham, Portable NMR with parallelism, *Anal. Chem.* 92 (2020) 2112–2120.
- [8] Y. Maguire, I.L. Chuang, S. Zhang, N. Gershenfeld, Ultra-small-sample molecular structure detection using microslot waveguide nuclear spin resonance, *Proc. Nat. Acad. Sci.* 104 (2007) 9198–9203.
- [9] S.G. van Meerten, K.C. Tijssen, P.J. van Bentum, A.P. Kentgens, \mathbf{B}_1 gradient coherence selection using a tapered stripline, *J. Magn. Reson.* 286 (2018) 60–67, <https://doi.org/10.1016/j.jmr.2017.11.004>.
- [10] R.C. Meier, J. Höflin, V. Badilita, U. Wallrabe, J.G. Korvink, Microfluidic integration of wirebonded microcoils for on-chip applications in nuclear magnetic resonance, *J. Micromech. Microeng.* 24 (2014) 045021.
- [11] S.S. Mohan, M. del Mar Hershenson, S.P. Boyd, T.H. Lee, Simple accurate expressions for planar spiral inductances, *IEEE J. Solid-state Circ.* 34 (1999) 1419–1424.
- [12] G.F. Pauli, B.U. Jaki, D.C. Lankin, Quantitative ^1H NMR: development and potential of a method for natural products analysis, *J. Nat. Prod.* 68 (2005) 133–149.
- [13] T.L. Peck, R.L. Magin, P.C. Lauterbur, Design and analysis of microcoils for NMR microscopy, *J. Magn. Reson., Series B* 108 (1995) 114–124.
- [14] M. Pellecchia, D.S. Sem, K. Wüthrich, NMR in drug discovery, *Nat. Rev. Drug Discovery* 1 (2002) 211–219.
- [15] P.B. Roemer, W.A. Edelstein, C.E. Hayes, S.P. Souza, O.M. Mueller, The NMR phased array, *Magn. Reson. Med.* 16 (1990) 192–225.
- [16] P.F. Silva, M. Jouda, J.G. Korvink, Geometrically-differential NMR in a stripline front-end, *J. Magn. Reson.* 310 (2020) 106659.
- [17] P.F. Silva, M.A. Jouzdani, M. Condesso, A.C.H. Rivera, M. Jouda, J.G. Korvink, Net-phase flow nmr for compact applications, *J. Magn. Reson.* 341 (2022) 107233.
- [18] C. Snyder, L. Delabarre, S. Moeller, J. Tian, C. Akgun, P.F. Van de Moortele, P. Bolan, K. Ugurbil, J. Vaughan, G. Metzger, Comparison between eight- and sixteen-channel TEM transceive arrays for body imaging at 7 T, *Magn. Reson. Med.* 67 (2012) 954–964.
- [19] E.G. Sorte, N.A. Banek, M.J. Wagner, T.M. Alam, Y.J. Tong, In situ stripline electrochemical NMR for batteries, *ChemElectroChem* 5 (2018) 2336–2340.
- [20] A.J. Oosthoek-de Vries, P.J. Nieuwland, J. Bart, K. Koch, J.W. Janssen, P.J.M. van Bentum, F.P. Rutjes, H.J. Gardeniers, A.P. Kentgens, Inline reaction monitoring of amine-catalyzed acetylation of benzyl alcohol using a microfluidic stripline nuclear magnetic resonance setup, *J. Am. Chem. Soc.* 141 (2019) 5369–5380.
- [21] H. Wang, L. Ciobanu, A. Edison, A. Webb, An eight-coil high-frequency probehead design for high-throughput nuclear magnetic resonance spectroscopy, *J. Magn. Reson.* 170 (2004) 206–212.